International Journal of Scientific Research in Engineering and Management (IJSREM)
Volume: 09 Issue: 04 | April - 2025 SJIF Rating: 8.586 ISSN: 2582-3930

Mechanical and Thermal Characterization of Nano-Al_2O_3 Fiber-Reinforced Polymer Composites: Fracture Analysis and Performance Evaluation

[1]Mrs. ARIPAKA JYOTHI (MTech Assistant professor), [1]B. LOKESH [1]B. SANKARA RAO, [1]B. JITHU VISHNUSAI, [1]B. VILAS GUNARAJA SEKHAR REDDY, [1]D. DHANU JAGAN.

[1]Department of Mechanical Engineering, Wellfare Institute of science Technology & Management, Visakhapatnam, India

Abstract

This study investigates the fabrication and characterization of nano-Al_2O_3 fiber-reinforced polymer composites using a hand lay-up technique. The composites consist of an epoxy/hardener matrix reinforced with E-glass fiber (610 GSM) and varying volume fractions (0–2.5%) of nano-Al_2O_3 powder synthesized via high-energy ball milling. Specimens are fabricated in accordance with ASTM D638 (tensile), ASTM D790 (flexural), and ASTM D785 (hardness) standards, employing a five-layer E-glass fiber laminate strucwture. Mechanical properties—tensile strength, flexural strength, and Rockwell hardness—are systematically evaluated and compared across Al_2O_3 volume percentages. Results highlight the influence of nano-Al_2O_3 reinforcement on enhancing mechanical performance, leveraging the inherent advantages of E-glass composites, such as high strength-to-weight ratio and wear resistance, for potential industrial applications.

Keywords: ultimate tensile strength, impact strength, hardness, DSC, DTA, TGA.

1. INTRODUCTION

Composite materials have been utilized since ancient times, evolving into modern lightweight, high-strength materials with exceptional mechanical, thermal, and electrical properties. Epoxy-based composites are widely used due to their high adhesion, chemical resistance, and ease of processing. This study focuses on fabricating Al_2O_3 nanoparticle-reinforced E-glass fiber polymer composites using a hand lay-up method. High-energy ball milling synthesizes nano-Al_2O_3 powder, which is incorporated into an epoxy matrix with varying volume fractions (0%, 0.5%, 1%, 1.5%, 2%, and 2.5%). Laminates are prepared with five layers of E-glass fiber and tested for tensile strength, flexural strength (three-point bending), and hardness following ASTM standards (ASTM D638, D790, D785). Results demonstrate significant improvements in mechanical properties with increasing reinforcement percentages, particularly at 2% and 2.5%. Nano-Al_2O_3 enhances tensile strength, fracture toughness, and stiffness due to its superior mechanical and thermal properties. Hybrid composites combining natural and synthetic fibers further optimize material performance for applications in aerospace, automotive, marine, construction, and electronics. Functionally graded materials with non-homogeneous microstructures enable tailored properties for advanced applications. This research highlights the potential of nano-Al_2O_3-reinforced polymer composites in industrial applications requiring high strength-to-weight ratios and durability.

2. Materials and method

2.1 Raw materials

Epoxy resin (LY 556) has been used as the matrix and hardener (HY951) as the curing agent. Chopped E-glass fiber and Al2O3 nanoparticles have been used as reinforcements.

2.2 Fabrication of composite

Historically, glass fiber-reinforced polymer (GFRP) composites have been fabricated using the hand lay-up technique. In this study, five-ply E-glass fiber mats were initially cut using scissors. A mixture of Al_2O_3 nanoparticles and plain

epoxy was manually blended for 10 minutes using a glass rod. The epoxy adhesive mixture was prepared by adding hardener at a ratio of 10:1 following thorough mixing of the epoxy.

The fabrication process involved positioning the first ply within a mold box, applying a coat of the epoxy adhesive mixture using a brush until complete saturation was achieved. Subsequent layers were added, allowing each to absorb the liquid before applying additional adhesive. This process was repeated until all five plies were stacked. A mild steel roller was used to remove excess adhesive and maintain uniform thickness across the composite surface.

Al_2O_3 powder was incorporated at varying concentrations (0%, 0.5%, 1%, 1.5%, 2%, and 2.5%), resulting in six distinct composite permutations. The composite laminates were cured at room temperature for 24 hours. Following curing, samples were cut from the laminates in accordance with ASTM standards for further mechanical testing.

2.3 Mechanical testing& Thermal analysis

The interfacial adhesion between the polymer matrix and glass fiber reinforcement is critical for determining the overall strength of glass fiber-reinforced polymer (GFRP) composites. These composites are characterized through comprehensive mechanical testing protocols. Specifically, the mechanical properties assessed include hardness, tensile strength, and flexural strength, while thermal properties are also evaluated to provide a holistic understanding of the composite's performance under various conditions.

2.3.1 Tensile testing

Tensile tests on the nanocomposites were conducted in accordance with ASTM D3039 standards. These tests were performed using a computerized universal testing machine at a controlled crosshead speed of 1 mm/min. All tensile evaluations were carried out at room temperature. A total of six samples were examined to ensure reliable and consistent results.

2.3.2 Flexural testing

The three-point flexural test was conducted using the same universal testing machine, adhering to the ASTM D790 standard. This test was employed to evaluate the flexural properties of the composites, providing insights into their bending behavior and resistance to deformation.

2.3.3 Hardness tests

The hardness of each composite sample was determined using a Rockwell hardness testing machine. This method provided a quantitative assessment of the surface hardness of the composites, offering valuable insights into their resistance to indentation and wear.

2.3.4Differential Scanning Calorimeter (DSC)

Differential scanning calorimetric (DSC) measurements were performed using a Mettler Toledo DSC calorimeter within a temperature range of 0°C to 350°C under atmospheric conditions. The melting and crystallization temperatures of the samples were determined midway through the thermal analysis process. This technique provided insights into the thermal transitions and phase changes of the materials under controlled heating conditions.

2.3.5 Derivative Thermal Analysis (DTA)

Differential thermal analysis (DTA) was performed using a Shimadzu TGA-50/DTA thermogravimetric analyzer. Under atmospheric conditions, samples were subjected to a controlled heating ramp from ambient temperature to 1000°C at a rate of 10°C/min. This technique facilitated the assessment of thermal transitions and phase changes within the material as a function of temperature.

2.3.6 Thermo gravimetric Analysis (TGA)

Thermogravimetric analysis (TGA) was conducted using a Shimadzu TGA-50 thermogravimetric analyzer. The samples were heated under atmospheric conditions at a controlled rate of 10°C/min, starting from ambient temperature and

progressing up to 1000°C. This method enabled the precise measurement of mass changes in the samples as a function of temperature, providing insights into their thermal stability, decomposition behavior, and physicochemical transitions

3. **Result & discussions**

3.1 Tensile test results

The influence of nano-Al_2O_3 particles on glass fiber-reinforced polymer (GFRP) composites is illustrated in Figure 1. The incorporation of nanoparticles significantly enhances the tensile strength of composite materials due to the strong interfacial bonding between the filler and matrix, as well as effective particle dispersion, which facilitates efficient stress transfer. The results indicate that the composite specimen reinforced with 1.5% nano-Al_2O_3 particles achieved the highest ultimate tensile strength of 248.99 MPa, exhibiting a more pronounced variation in tensile strength compared to other compositions. However, the ultimate tensile strength begins to decrease with the addition of 2% nano-Al_2O_3 particles, suggesting an optimal reinforcement concentration.

Table. 1 Ultimate tensile strength

Specimen	Ultimatetensilestrength(MPa)
A1	199
A2	207.55
A3	228.37
A4	248.99
A5	237.91
A6	182.96

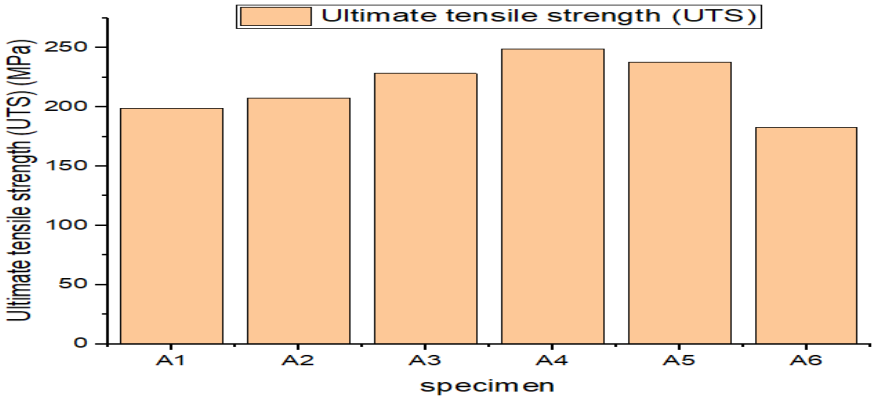

Fig.1: Variation of Tensile strength w.r.t Nano-Al2O3 Content in composites

3.2 Flexural test results

Figure 2 illustrates the flexural strength of composite samples with varying concentrations of nano-Al_2O_3 particles. The specimen reinforced with 1.5% nano-Al_2O_3 particles exhibited the highest flexural strength of 205.88 MPa, surpassing other composite specimens. This enhancement is attributed to the uniform dispersion of nano-fillers and the robust interfacial bonding between the epoxy matrix and the filler materials, which enhances energy absorption and effectively inhibits crack initiation and propagation. Furthermore, it is observed that the flexural strength of the composite specimens exhibits a steady increase as the fraction of nano-fillers increases, indicating a direct correlation between nano-filler content and improved flexural performance.

Table.2: Maximum Flexural strength.

Specimen	Maximum flexural strength(MPa)
A1	176.5
A2	186.2
A3	200.2
A4	205.88
A5	200.81
A6	205.63

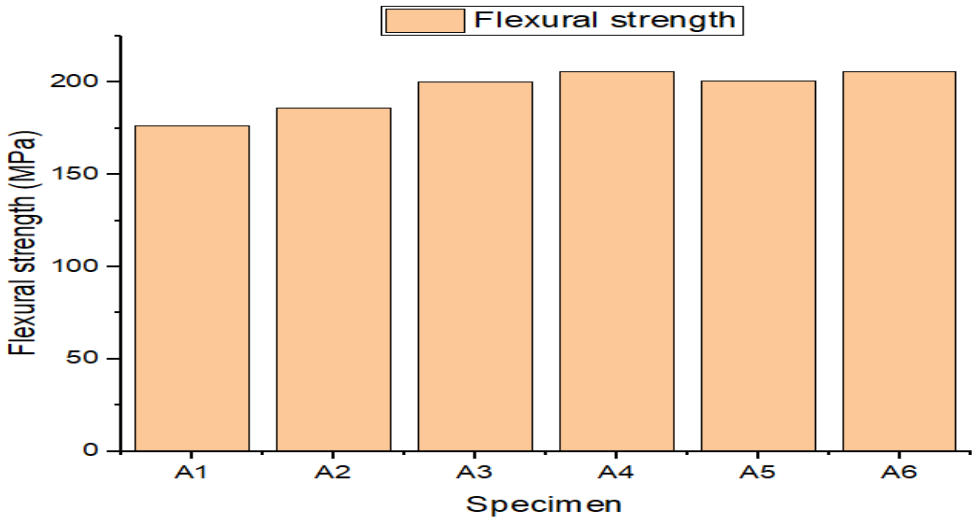

Fig.2: Variation of flexural strength w.r.t Nano-Al2O3 Content in composites

3.3 Hardness test results

The micro-hardness of the composite was evaluated using a digital Leco micro-hardness tester. A diamond indenter was applied to the composite specimen under a load of 3 N for a duration of 10 seconds to create an indentation. The typical Vickers hardness values are tabulated in Table 3 and Fig.3. The results indicate a gradual increase in hardness, with a maximum value of 25.3 Hv. However, the hardness values across different compositions show minimal variation, suggesting that the addition of nano-Al_2O_3 particles does not significantly impact the hardness of the composites.

Table. 3: Micro hardness values

Specimen	Micro Hardness Hv
A1	17.2
A2	18.5
A3	20.1
A4	21.6
A5	22.4
A6	25.3

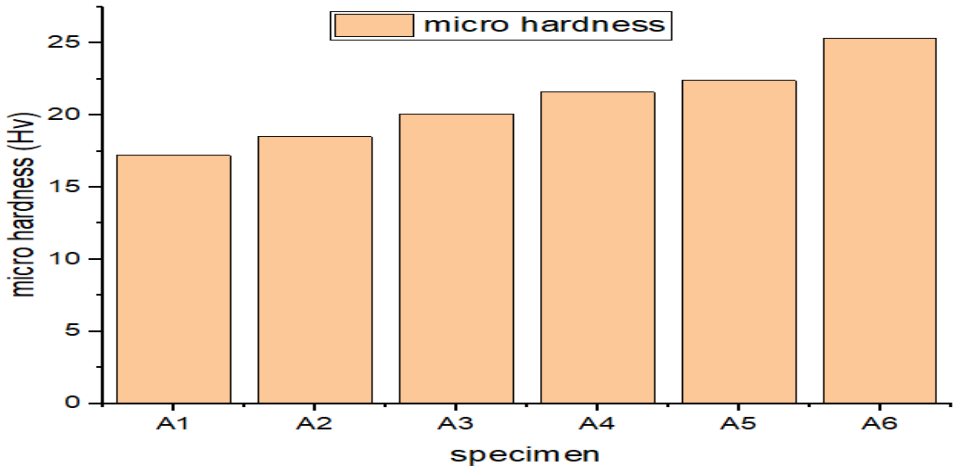

Fig.3: Variation of Hardness value w.r.t to nano-Al2O3 Content in composites.

3.4 DSC test results

The influence of micro-particles on the glass transition temperature (Tg) of the composite was analyzed across various compositions, specifically A1, A2, A3, A4, A5, and A6. The glass transition temperatures for these compositions with different modifiers are documented in Table 4 and Fig.4. The results indicate that there are no substantial variations in the Tg values, suggesting that the incorporation of micro-particles does not significantly alter the thermal transition behavior of the composites.

Table. 4: Glass transition temperature

Specimen	Glass transition temperature(°C)
A1	60.8
A2	61.6
A3	62.4
A4	63.6
A5	66.0
A6	67.5

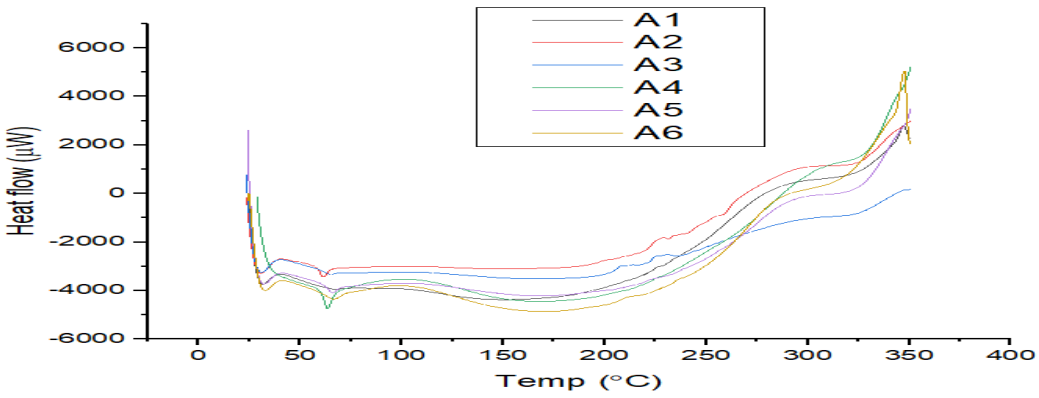

Fig.4: Temperature vs. Heat flow Graph

3.5 Derivative Thermal Analysis (DTA)

Figure 5 and Table 5 presents the differential thermal analysis (DTA) curves for nano-Al_2O_3 filler material composites in an oxygen atmosphere. The DTA peak in Fig.5 corresponds to the oxidation temperature of the Al_2O_3 nanocomposites, with a prominent spike observed at 474°C. This spike is attributed to the sudden mass loss of nano-Al_2O_3. Additionally, significant weight loss occurs between 400°C and 500°C, which is associated with the pyrolysis of polymer materials. A smaller weight loss is also observed between 600°C and 700°C, indicating further thermal degradation processes.

Table.5 Peak value temperature

Specimen	Peak value Temperature (°C)
A1	269
A2	423
A3	457
A4	464
A5	471
A6	474

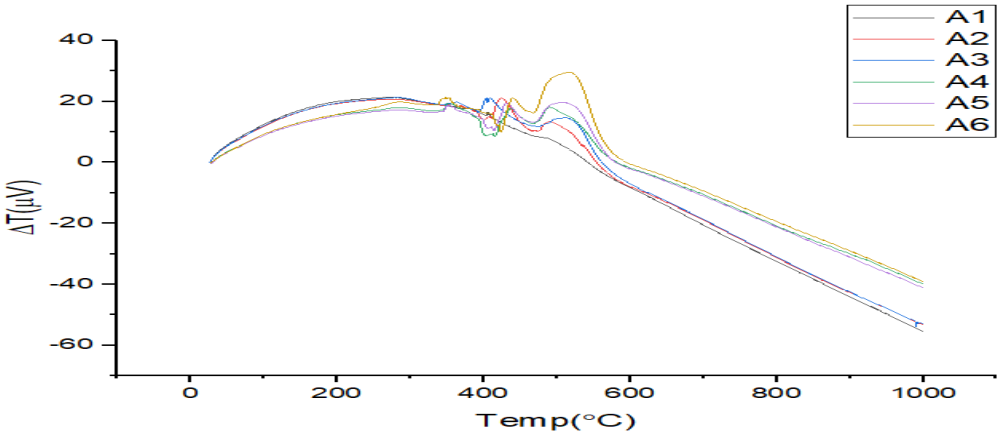

Fig.5: Temperature vs. Heat flow Graph

3.6 TGA test results

Table 6 outlines the initial and final temperatures of nano-Al_2O_3-filled composites. The incorporation of nanofillers into the polymer matrix enhances the thermal stability of the composites. The thermolysis process occurs in two stages: initially, the evaporation of interlayer moisture leads to composite degradation, with a 10% weight loss observed during this phase. The nano-Al_2O_3-filled composite undergoes degradation between 233°C and 257°C. In the second stage, thermal deterioration is influenced by factors such as filler loading, bonding strength, and filler-matrix compatibility. Notably, specimen A3 exhibits a higher weight loss percentage compared to A4, indicating that the 1.5% nano-Al_2O_3 composite (A4) is more thermally stable. Figure 6 illustrates that the ceramic nano-Al_2O_3 filler is more stable and robust than the epoxy matrix due to its heat-resistant properties. Consequently, the addition of nano-Al_2O_3 improves the thermal stability of polymer composites by enhancing their heat resistance. However, increasing the concentration of nano-Al_2O_3 results in decreased degradation temperatures, suggesting a complex relationship between filler content and thermal stability. Overall, nano-Al_2O_3 fillers contribute to improved thermal stability in polymer composites.

Table. 6: Initial and Final degradation temperatures

Specimen	Initial Degradation temperature(°C)	Final Degradation temperature(°C)
A1	233	573
A2	260	568
A3	265	582
A4	271	576
A5	280	562
A6	257	575

Fig.6 weight loss vs temperatures

4.**Fracture surface analysis through scanning electron microscopy (SEM)**

The underlying mechanisms of micro- and nanoscale failures in various composite sets can be elucidated through scanning electron microscopy (SEM) analysis of the fracture surfaces. Consequently, all composite specimens that failed during tensile testing underwent fractographic examinations to investigate the failure modes. The addition of nano-Al_2O_3 to epoxy is known to enhance the strength and toughness of specimens, which is expected to alter the typical failure mechanisms observed in conventional fiber-reinforced polymer (FRP) composites. This modification in failure behavior can provide valuable insights into the role of nano-Al_2O_3 in improving the mechanical performance of these composites.

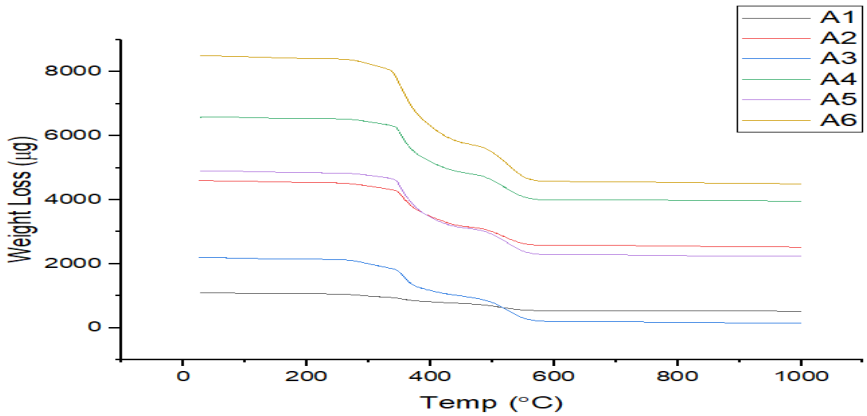

Figure.7:Fracture study of a 0.5% nano AL2O3 composite.

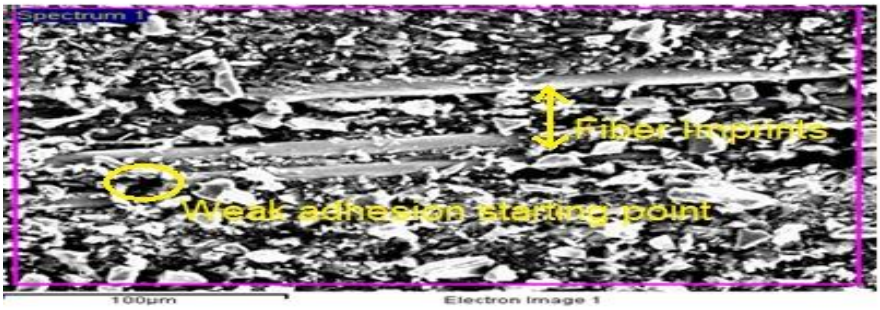

Figure 7 presents the delamination surfaces of the 0.5% nano-Al_2O_3 composites evaluated at room temperature. The morphology of the composite reveals smooth fiber impressions, indicative of delamination between the fibers and the polymer matrix. However, the incorporation of nano-Al_2O_3 alters the morphology of the fiber impressions. As depicted in Figure 7, all nano-Al_2O_3-reinforced composites exhibit matrix deformation and fiber impressions on the delaminated surface, suggesting an enhanced interaction between the fibers and the matrix due to the presence of nano-Al_2O_3 particles.

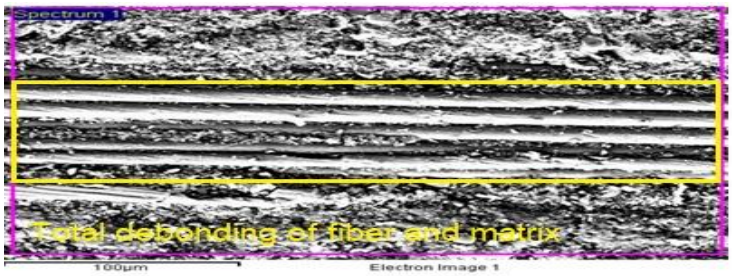

Figure.8: Analysis of 1.5% nano AL2O3 composite fracture.

Figure 8 illustrates the diverse deformation morphologies observed in the 1.5 weight percent nano-Al_2O_3 composites evaluated at room temperature. Specifically, the 1.5 wt% nano-Al_2O_3 composites exhibit fiber pull-out and hardening of the matrix phase, as shown in Figure 8. These features undoubtedly contribute to enhanced strength and modulus compared to control Al_2O_3 composites. In contrast, significant matrix deformation was observed in the control composites, as depicted in Figure 7. The presence of nano-Al_2O_3 particles in the 1.5 wt% composites leads to improved mechanical properties due to the enhanced interfacial interaction and matrix reinforcement.

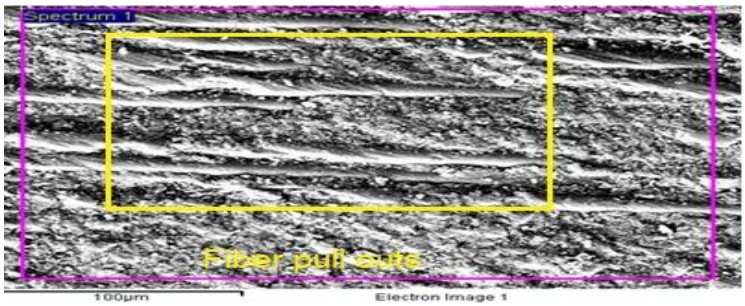

Figure .9:Fracture study of a 2.5% Nano AL2O3 composite.

Figure 9 displays a rough and bare fiber surface devoid of any polymeric phase, indicating fiber/matrix debonding that may be attributed to inadequate interfacial bonding. In contrast, the 0.5 weight percent nano-Al_2O_3 composite exhibits a coating of the epoxy matrix on the fibers' surface, suggesting a strong fiber/matrix interfacial bond. Additionally, the fiber surface in Figure 9 reveals characteristic morphologies such as mirror, mist, and hackle patterns, which are indicative of distinct failure modes and interfacial interactions. These observations highlight the role of nano-Al_2O_3 in

enhancing the interfacial adhesion between the fibers and the matrix, thereby influencing the composite's mechanical behavior.

5.Conclusions:

Experiments were conducted to evaluate the mechanical properties and dispersion stability of nano-Al_2O_3-reinforced epoxy composites by varying the volume percentage of nano-Al_2O_3. The mechanical characteristics of glass fiber-reinforced polymer laminates were enhanced by increasing the volume percentage of nano-Al_2O_3. Factors such as fiber orientation, nano-Al_2O_3 content, resin content, and fabrication technique influence laminate efficiency. However, issues related to stability, agglomeration, voids, and dispersion of nano-Al_2O_3 were encountered.

Various characterization instruments were employed to analyze the mechanical and microstructural behavior of nano-Al_2O_3-epoxy samples. Ultimate tensile strength, flexural strength, and microhardness were determined using a universal testing machine, a three-point bending test, and a tensile test, respectively. Thermal analysis was performed using DSC, DTA, and TGA tests. Scanning electron microscopy (SEM) was used to analyze the morphology of failed composite specimens, focusing on matrix epoxy and filler dispersion.

Mechanical Test Results:

Tensile Strength (ASTM D638): The tensile strengths for laminates with varying volume percentages of nano-Al_2O_3 (0%, 0.5%, 1%, 1.5%, 2%, and 2.5%) were 199 MPa, 207.55 MPa, 228.37 MPa, 248.99 MPa, 237.91 MPa, and 182.96 MPa, respectively. The 1.5 vol% nano-Al_2O_3 epoxy sample exhibited the highest tensile strength of 248.99 MPa. A decline in tensile strength was observed beyond 1.5 vol%, potentially due to nano-Al_2O_3 aggregation.

Flexural Strength (ASTM D790): Flexural strengths for laminates with varying volume percentages of nano-Al_2O_3 (0%, 0.5%, 1%, 1.5%, 2%, and 2.5%) were 176.5 MPa, 186.2 MPa, 200.2 MPa, 205.88 MPa, 200.81 MPa, and 205.63 MPa, respectively. The 1.5 vol% nano-Al_2O_3 epoxy sample achieved the highest flexural strength of 205.88 MPa. Similar to tensile strength, flexural strength decreased beyond 1.5 vol% due to possible aggregation.

Vickers Hardness (ASTM D785): The Vickers hardness values for laminates with varying volume percentages of nano-Al_2O_3 (0%, 0.5%, 1%, 1.5%, 2%, and 2.5%) were 17.2 Hv, 18.5 Hv, 20.1 Hv, 21.6 Hv, 22.4 Hv, and 25.3 Hv, respectively. The 2.5 wt% nano-Al_2O_3 epoxy sample had the highest Vickers hardness of 25.3 Hv. The increase in hardness beyond 1.5 vol% was attributed to enhanced brittleness, which compromised flexural and tensile strengths.

Thermal Analysis:

DSC: No significant changes were observed in the glass transition temperature (Tg) values.

TGA: A notable difference in weight loss was observed between samples A3 and A4, with A3 losing 90.5% more weight than A4, which lost 38.36%.

DTA: The peak values increased with the growth in nano-Al_2O_3 percentage, indicating changes in thermal behavior.

Overall, the addition of nano-Al_2O_3 improves the mechanical properties of epoxy composites up to a certain concentration, beyond which aggregation and increased brittleness may lead to decreased strength.

References

1. Andrews R and Weisenberger M C 2004 Carbon nanotube polymer composites. Current Opinion Solid State and Materials Science 8(1): 31–37
2. M.A.Megahed, A.A.Megahed, H.E.M.Sallam, U. A.Khashaba, M. A.Seif, M.Abd-Elhamid: Nano-reinforcement effects on tensile properties of epoxy resin, Proc. of the Int. Conf. MEATIP5, Assiut University, Egypt (2011), pp. 123–135Search in Google Scholar
3. Andrews R and Weisenberger M C 2004 Carbon nanotube polymer composites. Current Opinion Solid State and Materials Science 8(1): 31–37
4. Anish Khan, Sanjay MavinkereRangappa, Mohammad Jawaid, SuchartSiengchin, and Abdullah M. Asiri, Hybrid Fiber Composites: Materials, Manufacturing, Process Engineering - Google Books. 2020.
5. Saba, N.; Mohammad, F.; Pervaiz, M.; Jawaid, M.; Alothman, O.; Sain, M. Mechanical, morphological andstructural properties of cellulose nanofibers reinforced epoxy composites. Int. J. Biol. Macromol.2017,97,190–200.
6. M. Manjunath, N. M. Renukappa, and B. Suresha, "Influence of micro and nanofillers on mechanical properties of pultruded unidirectional glass fiber reinforced epoxy composite systems," J. Compos. Mater., vol. 50, no. 8, pp. 1109–1121, 2016
7. Romano, M.; Goldie, B.; Kehr, A.; Roche, M.; Papavinasam, S.; Attard, M.; Balducci, B.; Revie, R.W.; Melot, D.; Paugam, G. Protecting and Maintaining Transmission Pipeline. J. Prot. Coat. Linings e-book 2012. [Google Scholar]
8. Popov, B.N. Organic coatings. In Corrosion Engineering—Principles and Solved Problems; Elsevier: Amsterdam, The Netherlands, 2015; ISBN 9781420094633. [Google Scholar]
9. Kandelbauer, A. Processing. In Handbook of Thermoset Plastics, 3rd ed.; Dodiuk, H., Goodman, S. H., Eds.; William Andrew, 2014; pp 739– 753.[Crossref], Google Scholar
10. Islam M., Ar-Rashid H., Islam F., Karmaker N., Koly F.A., Mahmud J., Keya K.N., Khan R.A. *Nano Hybrids and Composites.* Volume 24. Trans Tech Publications Ltd.; Pfaffikon, Switzerland: 2019. Fabrication and Characterization of E-Glass Fiber Reinforced Unsaturated Polyester Resin Based Composite Materials; pp. 1–7. [Google Scholar]
11. Sarkar P, Modak N, Sahoo P (2018) Effect of aluminum filler on friction and wear characteristics of glass epoxy composites. Silicon 10(3):715–723
12. Suresh S, Mortensen A (1998) Fundamentals of functionally graded materials: processing and thermomechanical behaviour of graded metals and metal-ceramic composites. The Institute of Materials, IOM Communications Ltd, London
13. Asi, O. "An experimental study on the bearing strength behavior of Al2O3 particle filled glass fiber reinforced epoxy composites pinned joints," Composite Structures, V. 92, No. 2, 2010, pp. 354– 63.
14. K.K. Mahato *et al.*Effect of loading rates of severely thermal-shocked glass fiber/epoxy composites Compos Commun (2017)
15. M.M. Shokrieh *et al.* Tension behavior of unidirectional glass/epoxy composites under different strain rates Compos Struct (2009)
16. F. Shehata, A. Fathy, M. Abdelhameed, S.F. MoustafaPreparation and properties of Al_2O_3 nanoparticle reinforced copper matrix composites by in situ processing Mater Des, 30 (7) (2009), pp. 2756-2762.
17. Biercuk MJ, Llaguno MC, Radosvljevic M, Hyun JK, Johnson AT. Carbon nanotube composites for thermal management. ApplPhys Lett 2002;80:15.
18. Ounaies Z, Park C, Wise KE, Siochi EJ, Harrison JS. Electrical properties of single wall carbon nanotube reinforced polyimide composites. Compos SciTechnol 2003;63:1637–46, This work describes SWNT polyimide composites with low percolation thresholds and conductivities exceeding that needed for antistatic applications.
19. Omrani, L. C. Simon, A. A. Rostami, Mater. Chem. Phys. 2009, 114, 145.

20. E Mader *et al.*Surface, interphase and composite property relations in fiber-reinforced polymers **Composites**(1994)

21. G. Prokopski *et al.***Effect of water/cement ratio and silica fume addition on the fracture toughness and morphology of fractured surfaces of gravel concretes** Cem. Concr. Res.(2000)

22. Minh-Tai Le and Shyh-Chour Huang (2015) "Thermal and mechanical behavior of hybrid polymer nanocomposite reinforced with graphene nanoplatelets." Materials, 8, 5526-5536.

23. Alexandre M, Dubois P (2000) Polymer-layered silicate nanocomposites: preparation, properties and uses of a new class of materials. Mater SciEng R Rep 28:1–63. doi:10.1016/S0927-796X(00)00012-7

24. Zhao S, Schadler LS, Duncan R, Hillborg H, Auletta T (2008) Mechanisms leading to improved mechanical performance in nanoscale Al_2O_3 filled epoxy. Compos SciTechnol 68:2965–2975

25. Suri, K., Annapoorni, S., Tandon, R. &Mehra, N., 2002. Nanocomposite of polypyrrole-iron oxide by simultaneous gelation and polymerization. *Synthetic Metals, 126* (2-3)**,** pp.137-142.

26. Zhao Hongxia, Robert K.Y. Li, 2008. Effect of water absorption on the mechanical and dielectric properties of nano-alumina filled epoxy nanocomposites. Composites Part A 39, 602–611

27. Bakar, N.H., Hyie, K.M., Ramlan, A.S,, Hassan, M.K, and Jumahat, A. Mechanical Properties of Kevlar Reinforcement in Kenaf Composites. Applied Mechanics and Materials. 465-466: 847-851. . 2014.